Minimum acceleration with constraints of center of mass: a unified model for arm movements and object manipulation

Raz Leib and Amir Karniel

J Neurophysiol 108:1646-1655, 2012. First published 13 June 2012;
doi: 10.1152/jn.00224.2012

J Neurophysiol 108: 1646–1655, 2012.
First published June 13, 2012; doi:10.1152/jn.00224.2012.

Minimum acceleration with constraints of center of mass: a unified model for arm movements and object manipulation

Raz Leib and Amir Karniel

Biomedical Engineering Department, Ben-Gurion University of the Negev, Beer-Sheva, Israel

Submitted 15 March 2012; accepted in final form 13 June 2012

Leib R, Karniel A. Minimum acceleration with constraints of center of mass: a unified model for arm movements and object manipulation. *J Neurophysiol* 108: 1646–1655, 2012. First published June 13, 2012; doi:10.1152/jn.00224.2012.—Daily interaction with the environment consists of moving with or without objects. Increasing interest in both types of movements drove the creation of computational models to describe reaching movements and, later, to describe a simplified version of object manipulation. The previously suggested models for object manipulation rely on the same optimization criteria as models for reaching movements, yet there is no single model accounting for both tasks that does not require reminimization of the criterion for each environment. We suggest a unified model for both cases: minimum acceleration with constraints for the center of mass (MACM). For point-to-point reaching movement, the model predicts the typical rectilinear path and bell-shaped speed profile as previous criteria. We have derived the predicted trajectories for the case of manipulating a mass-on-spring and show that the predicted trajectories match the observations of a few independent previous experimental studies of human arm movement during a mass-on-spring manipulation. Moreover, the previously reported "unusual" trajectories are also well accounted for by the proposed MACM. We have tested the predictions of the MACM model in 3 experiments with 12 subjects, where we demonstrated that the MACM model is equal or better (Wilcoxon sign-rank test, $P < 0.001$) in accounting for the data than three other previously proposed models in the conditions tested. Altogether, the MACM model is currently the only model accounting for reaching movements with or without external degrees of freedom. Moreover, it provides predictions about the intermittent nature of the neural control of movements and about the dominant control variable.

reaching movement; Pontryagin's minimum principle; optimal control

CONSIDER A WAITER SERVING a full cup of coffee and his colleague reaching to grasp and lift an empty cup. Clearly, the tasks are different, because the first requires more dexterity than the second; however, the brain may employ similar principles in the motor planning of both tasks. In the motor control research, a simplified version of the second task is the well-studied unconstrained reaching movement (Abend et al. 1982; Flash and Hogan 1985; Morasso 1981), whereas a simplified version of the first task is the manipulation of mass-on-spring (see Fig. 1) during reaching movement (Dingwell et al. 2002).

It was hypothesized that smoothness is a primary goal of the motor system. According to this hypothesis, optimization criteria were suggested for reaching, e.g., minimum hand jerk (Flash and Hogan 1985), and later for object manipulation, e.g., minimum object crackle (MOC) (Dingwell et al. 2004), minimum hand jerk (MHJ), and minimum hand driving force change (MHFC) (Svinin et al. 2005).

Although providing logical solutions for object manipulation, as detailed in METHODS, the MOC (Dingwell et al. 2004; Huegel et al. 2009; Svinin et al. 2006) and MHJ models (Svinin et al. 2005) do not fit well to experimental data for some mass and spring values. Moreover, the MOC model is specific to the mass-on-spring task and cannot be extended to multiple masses (Svinin et al. 2006), whereas the solution of MHFC for reaching movements may be unstable because it is a numeric solution calculated using an iterations scheme.

The common feature for all criteria is the need to reminimize the criteria under the dynamic constraints imposed by the environment, e.g., for reaching, simple object manipulation, or complex object manipulation, i.e., multiple masses. Therefore, we have developed a single model that covers all these cases without reminimization of the criterion based on the environment.

Recently, a model based on minimizing hand acceleration was proposed to account for reaching movements. This model suggested minimizing hand acceleration while constraining the maximum value of hand jerk (Ben-Itzhak and Karniel 2008). The minimization results in a three-part constant intermittent control signal, which depends on the jerk constraint. The ability to account for experimental results (Berret et al. 2011), the prediction of intermittence control, and the biological reasoning of sensing and computing acceleration make this model a serious candidate to explain the nature of reaching movements.

Most studies of reaching movements have concentrated on hand trajectory. Suzuki et al. (1997) questioned the role of the endpoint during reaching planning: while considering the complex configuration of the hand, comparison of reaching movements between different points revealed that although the endpoint trajectory may be altered, the hand center-of-mass (CoM) trajectory remains invariant, emphasizing the important role of the CoM in planning reaching movements.

In this study we propose a single smoothness minimization criterion to account for reaching movements with or without external degrees of freedom, a minimum acceleration of the center of mass (MACM). We derive the prediction of the MACM for the CoM trajectory of a mass-on-spring. We demonstrate that our model accounts for previously reported trajectories, including trajectories unaccountable by other criteria. Moreover, we report new experimental results demonstrating the superiority of our model.

Address for reprint requests and other correspondence: A. Karniel, Biomedical Engineering Dept., Ben-Gurion Univ. of the Negev, Ben-Gurion 1, Beer-Sheva, Israel (e-mail: akarniel@bgu.ac.il).

METHODS

Object Manipulation Task

We used the same task as originally suggested by Dingwell et al. (2002). The task consists of transporting a mass-on-spring attached to the hand from an initial point to a target point in the horizontal plane (Fig. 1). This environment sets the following dynamics derived from Newton's Second Law: an object motion equation,

$$k(x_h - x_o) = m_o\ddot{x}_o \tag{1}$$

and a hand motion equation,

$$F + k(x_o - x_h) = m_h\ddot{x}_h \tag{2}$$

where F indicates the forces the hand is generating during movement.

The primary objective of transferring both hand and object between points sets 12 boundary conditions that depend on the movement duration, T, and movement length, L. For the hand,

$$\begin{aligned} x_h(t=0) &= 0, \quad \dot{x}_h(t=0) = \ddot{x}_h(t=0) = 0 \\ x_h(t=T) &= L, \quad \dot{x}_h(t=T) = \ddot{x}_h(t=T) = 0 \end{aligned} \tag{3a}$$

For the object,

$$\begin{aligned} x_o(t=0) &= 0, \quad \dot{x}_o(t=0) = \ddot{x}_o(t=0) = 0 \\ x_o(t=T) &= L, \quad \dot{x}_o(t=T) = \ddot{x}_o(t=T) = 0 \end{aligned} \tag{3b}$$

To capture the smoothness character for movement with the object, the problem was defined as an optimization problem in which a cost function of state variables is minimized (Dingwell et al. 2004; Flash and Hogan 1985; Hogan 1984). The minimization is achieved by using the Euler-Poisson equation, resulting in an expression for object position. To get the hand position, the different expressions for the object position are substituted into the object motion equation (*Eq. 1*).

Minimum object crackle model. Dingwell et al. (2004) suggested minimizing the fifth derivative of an object's position, the object crackle:

$$\int_0^T \left[\frac{d^5(x_o)}{dt^5}\right]^2 dt \tag{4}$$

The resulting object position model depends on the movement duration and movement length. After substituting the expression for object position into *Eq. 1*, we get the resulting hand position model, which depends on the ratio between object mass and spring constant as well as on the movement length and duration. The solution for minimizing this criterion indeed satisfies the boundary conditions (*Eq. 3*) and can be considered to be a reasonably descriptive model for the object manipulation task.

As discussed by Dingwell et al. (2004), if the ratio between object mass and spring remains constant, the model predicts identical hand kinematics. As described below, we have designed three experimental conditions to test this prediction.

To describe reaching movements, we can change the criteria, for example, minimization of hand crackle. However, for more complex environments, such as a chain of masses-on-springs, the minimum object crackle (MOC) does not satisfy the boundary conditions, requiring higher order derivatives for the optimization criterion (Svinin et al. 2006). Altogether, the MOC model seems to be specific to the mass-on-spring task because it needs to be altered according to the task and environment, resulting in different criteria defined in different sets of coordinates (hand or object) while using different derivative orders (e.g., crackle, snap, or higher derivatives).

Minimum hand jerk model. Another criterion, suggested by Svinin et al. (2005, 2006), is the minimum hand jerk (MHJ) model, minimizing the hand position third derivative:

$$\int_0^T \left[\frac{d^3(x_h)}{dt^3}\right]^2 dt \tag{5}$$

This criterion was used to describe unconstrained reaching movements (Flash and Hogan 1985); however, for object manipulation tasks, the object motion equation (*Eq. 1*) must be used, transforming the criterion in *Eq. 5* to

$$\int_0^T \left[\frac{m_o}{k}\frac{d^5(x_o)}{dt^5} + \frac{d^3(x_o)}{dt^3}\right]^2 dt \tag{6}$$

The resulting hand position model depends on the ratio between object mass and spring constant as well as on the movement length and duration. Similar to the MOC model, the hand kinematics predicted by this model will not change as long as the object mass-spring ratio is kept constant.

Although the optimization criterion does not change between the two tasks of simple reaching and object manipulation, there is a need for reminimization of the criterion for each of these tasks and

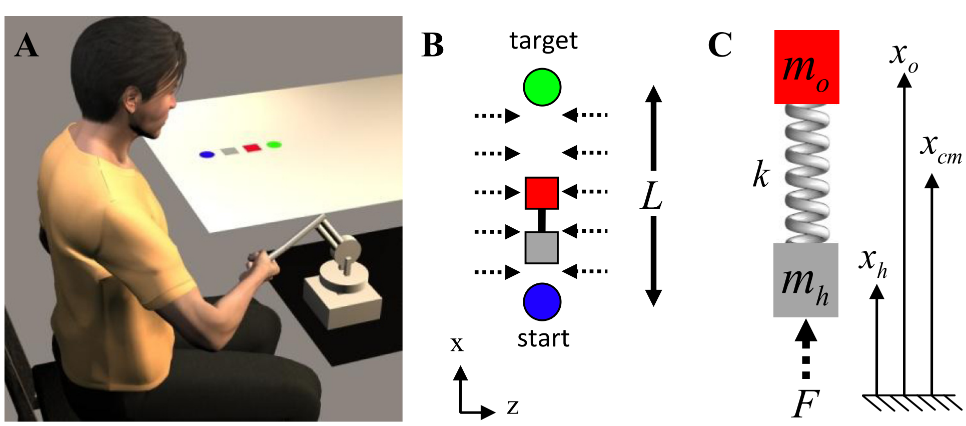

Fig. 1. Experimental setup. *A*: haptic device setup. The subject looks at a projection of the experiment from a projector located overhead while holding the handle of a robotic haptic device. *B*: the visual display used in the experiment. The blue disk represents the initial moving point, the green disk represents the target point, the gray square represents the subject's hand, and the red square represents the object. *L* is the distance between the initial point and the target, and the dashed arrows represent the orthogonal forces keeping the movement within a 1-dimensional channel. *C*: diagram of the hand as a point mass, m_h, and the simulated mass, m_o, attached (virtually) to the hand by a spring with constant k. The hand position is denoted by x_h, and the object position is denoted by x_o. F indicates the forces the hand is generating during movement. The center of mass (x_{cm}) is derived as a weighted sum of the hand position and the object position.

again for more complex objects. Moreover, this criterion could not account for some of the previous experimental results, in the sense of accurate prediction of the number of phases exhibited during movement, as demonstrated in the work of Svinin et al. (2005).

Minimum hand driving force change model. A third model, suggested by Svinin et al. (2005), considers the force the hand is producing during movement with the object, F. This variable is an equivalent representation of the joint torque as suggested by Uno et al. (1989).

According to this model, the optimal trajectory is found by minimizing the square changes in force:

$$\int_0^T \left[\dot{F}\right]^2 dt \tag{7}$$

The suggested cost function is then transformed using the hand motion equation (*Eq. 2*) and object motion equation (*Eq. 1*):

$$\int_0^T \left[\frac{m_h m_o}{k}\cdot\frac{d^5(x_o)}{dt^5} + (m_h + m_o)\cdot\frac{d^3(x_o)}{dt^3}\right]^2 dt \tag{8}$$

This model also depends on the hand mass value, unlike models resulting from the criteria described in *Eqs. 4* and *5*, in addition to the dependency on the object mass, spring constant, and movement length and duration. Unlike in previous models, keeping the object mass-spring ratio constant while changing each parameter value will create different predictions of hand kinematics in this model.

The criterion in *Eq. 7* can also be used to describe unconstrained reaching movements. Unlike the process of transferring this criterion (*Eq. 7*) to the criterion for object manipulation (*Eq. 8*), for reaching movement there is no need of such transformation. Without an external object, the optimization problem needs to be resolved according to the criterion in *Eq. 7*, and not the criterion in *Eq. 8*; i.e., there is a need to find the optimal trajectory by reminimization of the criterion. As shown by Svinin et al. (2005), the solution for minimizing this criterion for unconstrained reaching movement is a numerical one similar to the iterative scheme solution of the minimum joint torque-change model (Uno et al. 1989). As suggested in the same study, the solution is not guaranteed because it may not converge. Extending the criterion to more complex environments is done in a similar way to the MHJ model, suggesting that there is a need to reminimize the criterion for each environment and task.

Minimum acceleration with constraints applied to the center of mass. We propose to examine a state variable that combines both hand and object, namely, the system CoM. As in previous studies where the hand complex configuration and dynamics are ignored and the hand is considered as a point mass, the system CoM is defined as

$$x_{cm} = \frac{m_h x_h + m_o x_o}{m_h + m_o} \tag{9}$$

This assumption overlooking the complex dynamics of the hand and treating it as a point mass is not new (Svinin et al. 2005) and serves as a first approximation of the hand. Moreover, because the feedback given to the subject in this and previous studies is a visual point at the location of the hand, the subject is not required to control hand configuration.

To achieve smooth trajectory of the hand and object, we minimize the CoM acceleration from an initial to a final position in a given time T:

$$\int_0^T \left[\ddot{x}_{cm}\right]^2 dt \tag{10}$$

To solve the optimization problem, we suggest using the solution of the minimum acceleration with constraints criterion (MACC) for reaching movements (Ben-Itzhak and Karniel 2008). This will provide us with a description of the CoM trajectory, thus solving the optimization problem for the mass-on-spring system. By using this solution, derived for unconstrained reaching movements, we do not need to resolve the optimization problem given the new environment. The position of the CoM is given by

$$\begin{gathered}
x_{cm} = \begin{cases} \frac{1}{6}{}^1c_0t^3 - \frac{1}{2}{}^1c_1t^2 + {}^1c_2t + {}^1c_3, & 0 \le t \le t_1 \\ \frac{1}{6}{}^2c_0t^3 - \frac{1}{2}{}^2c_1t^2 + {}^2c_2t + {}^2c_3, & t_1 \le t \le t_2 \\ \frac{1}{6}{}^3c_0t^3 - \frac{1}{2}{}^3c_1t^2 + {}^3c_2t + {}^3c_3, & t_2 \le t \le T \end{cases} \\
{}^1c_0 = u \quad {}^1c_1 = {}^1c_2 = {}^1c_3 = 0 \\
{}^2c_0 = \frac{-24uL}{uT^3 - 24L + \sqrt{uT^3(uT^3 - 24L)}} \\
{}^2c_1 = \frac{-12uLT}{uT^3 - 24L + \sqrt{uT^3(uT^3 - 24L)}} \\
{}^2c_2 = \frac{(12L - uT^3)\sqrt{uT} + uT^2\sqrt{uT^3 - 24L}}{4\sqrt{uT^3 - 24L}} \\
{}^2c_3 = \frac{(6L - uT^3)\sqrt{uT^3 - 24L} + (uT^3 - 18L)\sqrt{uT^3}}{12\sqrt{uT^3 - 24L}} \\
{}^3c_0 = u \quad {}^3c_1 = uT \quad {}^3c_2 = \frac{1}{2}uT^2 \quad {}^3c_3 = L - \frac{1}{6}uT^3 \\
t_1 = \frac{T}{2}\left(1 - \sqrt{\frac{u\cdot T^3 - 24\cdot L}{u\cdot T^3}}\right) \\
t_2 = \frac{T}{2}\left(1 + \sqrt{\frac{u\cdot T^3 - 24\cdot L}{u\cdot T^3}}\right)
\end{gathered} \tag{11}$$

This analytical solution provides a descriptive model of the CoM trajectory. This description is divided into three time intervals. The position of the CoM in each time interval is given by a polynomial and its related coefficients, ${}^ic_j$, where i is time interval index and j is the coefficient number index. As discussed in detail in the original article (Ben-Itzhak and Karniel 2008), this model suggested minimizing the acceleration while constraining the maximum value of the jerk, u. The model is derived using Pontryagin's minimum principle, resulting in a three-part constant intermittent control signal, which depends on the jerk constraint, u, providing a prediction about the intermittent nature of the control signal.

Extracting the object position from *Eq. 9* and substituting in *Eq. 1*, we obtain the following ordinary differential equation linking the hand position and its derivatives to the CoM position and its derivatives:

$$\begin{gathered}
\ddot{x}_h + \beta x_h = \alpha\ddot{x}_{cm} + \beta x_{cm} \\
\beta = k\left(\frac{m_o + m_h}{m_h m_o}\right) = \omega^2 \\
\alpha = \left(1 + \frac{m_o}{m_h}\right)
\end{gathered} \tag{12}$$

To get the hand position, we simply need to solve the above ordinary differential equation. Because the CoM position is divided into three time intervals (*Eq. 11*), the solution of the hand position will also be divided into three time intervals:

$$x_h(t) = \begin{cases} A_1^1\cos(\omega t) + A_2^1\sin(\omega t) + \frac{1}{6}{}^1c_0t^3 - \frac{1}{2}{}^1c_1t^2 + \frac{{}^1c_2\beta + {}^1c_0(\alpha-1)}{\beta}t + \frac{{}^1c_3\beta - {}^1c_1(\alpha-1)}{\beta}, & 0 \le t \le t_1 \\ A_1^2\cos(\omega t) + A_2^2\sin(\omega t) + \frac{1}{6}{}^2c_0t^3 - \frac{1}{2}{}^2c_1t^2 + \frac{{}^2c_2\beta + {}^2c_0(\alpha-1)}{\beta}t + \frac{{}^2c_3\beta - {}^2c_1(\alpha-1)}{\beta}, & t_1 \le t \le t_2 \\ A_1^3\cos(\omega t) + A_2^3\sin(\omega t) + \frac{1}{6}{}^3c_0t^3 - \frac{1}{2}{}^3c_1t^2 + \frac{{}^3c_2\beta + {}^3c_0(\alpha-1)}{\beta}t + \frac{{}^3c_3\beta - {}^3c_1(\alpha-1)}{\beta}, & t_2 \le t \le T \end{cases} \tag{13a}$$

where

$$\begin{aligned} A_1^1 &= 0 \\ A_2^1 &= -\frac{{}^1c_0(\alpha-1)}{\beta\omega} \\ A_1^2 &= \frac{(a-1)\cdot\left[{}^3c_0\cdot\sin(\omega T-\omega t_2)\cdot\sin(\omega t_1)+{}^1c_0\cdot\sin(\omega t_2)\cdot\sin(\omega t_1)\right]}{\beta\omega\,\sin(\omega(t_1-t_2))} \\ A_2^2 &= -\frac{\left[{}^1c_0\cdot\cos(\omega t_2)\cdot\sin(\omega t_1)-{}^3c_0\cdot\cos(\omega T)\cdot\cos(\omega t_1)\cdot\sin(\omega t_2)\right]\cdot(a-1)}{\beta\omega\,\sin\left[\omega(t_1-t_2)\right]} - \frac{\left[{}^3c_0\cdot\sin(\omega T)\cdot\cos(\omega t_1)\cdot\cos(\omega t_2)\right]\cdot(a-1)}{\beta\omega\,\sin\left[\omega(t_1-t_2)\right]} \\ A_1^3 &= -\frac{{}^3c_0\cdot\sin(\omega T)\cdot(\alpha-1)}{\beta\omega} \\ A_2^3 &= -\frac{{}^3c_0\cdot\cos(\omega T)\cdot(\alpha-1)}{\beta\omega} \end{aligned} \tag{13b}$$

$$\sum_{k=0}^{7}\frac{(-1)^k}{(2k+1)!}\left(\omega\cdot\frac{T}{2}\sqrt{\frac{uT^3-24L}{uT^3}}\right)^{2k} = \frac{\sin\left(\omega\cdot\frac{T}{2}\right)}{\omega\cdot\frac{T}{2}}$$

The model depends on the object mass, spring constant, and movement length and duration, as well on the hand mass value.

We have derived this solution using standard methods for finding the homogenous solution by solving the characteristic equation and then, for each time interval, using the method of undetermined coefficient to find a particular solution (for an explanation of the method, see Boyce and DiPrima 1970). It is interesting to note that during this procedure, we had initially six boundary conditions and six continuity conditions; however, five were redundant, namely, identical to one of the other seven conditions, and therefore we were left with seven equations and seven parameters to obtain the single solution in *Eq. 13*. Nevertheless, because an ordinary differential equation has a unique solution, one can simply substitute our solution into the *Eq. 12* to prove it. These seven parameters are the six undetermined coefficients A_1^1, A_2^1, A_1^2, A_2^2, A_1^3, A_2^3 and the jerk constraint, u. The expression for the last parameter is not given explicitly because it is a complex expression that contains many terms; however, one can simply solve the high-order polynomial equation by factoring the polynomial or using numeric methods such as the Newton method.

A basic requirement of any model is to provide a logical description for 1-degree-of-freedom object manipulation while using extreme values of the mass and spring. This can be achieved while changing the spring and mass values to create different manipulation scenarios. For example, when the movement is performed without the additional mass, i.e., $m_o = 0$, $k = 0$, the model describing the hand trajectory converges to the MACC model, as expected, to describe this simple reaching movement. Another case is when $k \to \infty$, which can be considered as moving while holding a rigid object; the model again converges to the MACC model, as expected, because the object position coincides with the hand position.

Phase analysis of the MACM velocity profiles. To design the experiment and test the predictions of the various models, we have analyzed the expected velocity profiles and in particular the local minima and maxima values. Changes between local maximum and minimum speed values or vice versa are referred to as phase transitions (Svinin et al. 2006). This analysis is performed on simulation results of the model predictions provided by *Eq. 13*. Because the MACM model predictions depend on the system parameters spring constant, external mass, hand mass, movement length, and duration, we could not create a single illustration capturing the effect each parameter has on the velocity profile. To find how changes in a particular constant value affect the number of phases, one can construct a two-variable function of the hand velocity that depends on time and the constant in question. For example, we illustrated the velocity profiles as a function of the hand mass while keeping a fixed value of the other constants (Fig. 2).

Finding the saddle points in such illustrations will provide the critical value at which phase transition occurs. These saddle points satisfy the condition where both the acceleration and jerk become zero (Dingwell et al. 2004; Svinin et al. 2005):

$$\begin{aligned} \ddot{x}_h(t) &= 0 \\ \dddot{x}_h(t) &= 0 \end{aligned} \tag{14}$$

The velocity extremum is found by setting its derivative to zero, i.e., finding at which time points the acceleration is equal to zero. After finding these critical points, we want to decide whether there is a local maximum, minimum, or saddle point. This is done by calculating the

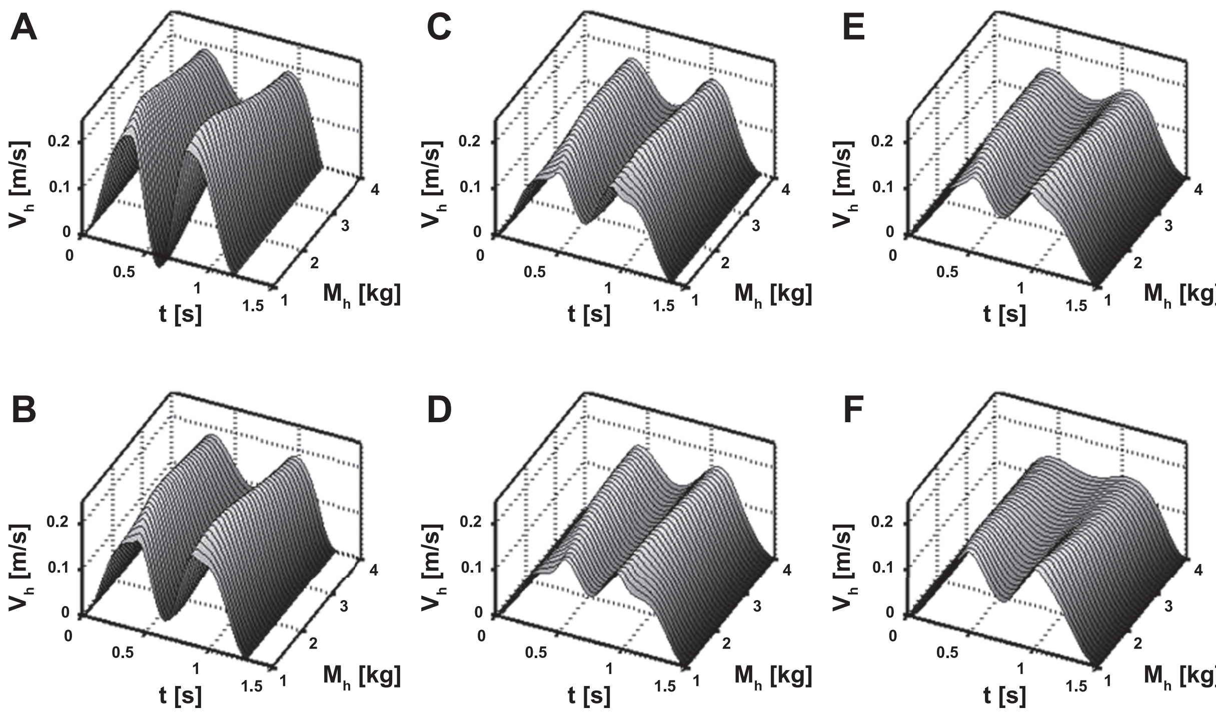

Fig. 2. Predictions of the minimum acceleration of center-of-mass (MACM) model. *A–D*: examples of the hand velocity (V_h) profiles predicted by the MACM model for transporting the mass-on-spring, a 4-kg object with a spring stiffness equal to 120 N/m, while the hand mass (m_h) was increased from 1 to 4 kg. The movement duration (T) increased between panels: in *A*, $T = 1.2$ s; in *B*, $T = 1.3$ s; in *C*, $T = 1.4$ s; and in *D*, $T = 1.5$ s. *E* and *F*: examples of the hand velocity profiles predicted by the MACM model for transporting the mass-on-spring where the movement duration remained constant while the hand mass was increased from 1 to 4 kg. The spring and mass values were changed between panels: in *E*, a 3-kg object and 90 N/m spring; in *F*, a 2-kg object and 60 N/m spring. For the selected constants used in these examples, the phase analysis did not show any change in the number of phases, which remains 2.

second derivative of velocity at these points. If the jerk is zero, this is a saddle point; otherwise, it is a local minimum or maximum (Apostol 1967). This phase analysis can be performed using the second and third derivative of the simulated hand position provided in *Eq. 13*.

Extension of the MACM Model to More Complex Environments

To further examine the abilities of the MACM model and its advantage over previous models, we considered two parallel mass-on-spring objects attached to the hand (Fig. 3) and demonstrated that the MHJ and MOC models cannot be extended to account for this case. This environment sets the following dynamics: the motion equation of the first mass, m_1,

$$m_1\ddot{x}_1 = k_1(x_h - x_1) \tag{15}$$

the motion equation of the second mass, m_2,

$$m_2\ddot{x}_2 = k_2(x_h - x_2) \tag{16}$$

and the motion equation of the hand, m_h,

$$m_h\ddot{x}_h = F + k_1(x_1 - x_h) + k_2(x_2 - x_h) \tag{17}$$

where boundary conditions for the task are as follows: for the hand,

$$\begin{aligned} x_h(t=0) = 0, \dot{x}_h(t=0) = 0, \ddot{x}_h(t=0) = 0 \\ x_h(t=T) = L, \dot{x}_h(t=T) = 0, \ddot{x}_h(t=T) = 0 \end{aligned} \tag{18}$$

for the first object,

$$\begin{aligned} x_1(t=0) = 0, \dot{x}_1(t=0) = 0, \ddot{x}_1(t=0) = 0 \\ x_1(t=T) = L, \dot{x}_1(t=T) = 0, \ddot{x}_1(t=T) = 0 \end{aligned} \tag{19}$$

and for the second object,

$$\begin{aligned} x_2(t=0) = 0, \dot{x}_2(t=0) = 0, \ddot{x}_2(t=0) = 0 \\ x_2(t=T) = L, \dot{x}_2(t=T) = 0, \ddot{x}_2(t=T) = 0 \end{aligned} \tag{20}$$

Minimum hand jerk. As suggested by (Svinin et al. 2006), to create a descriptive model using the MHJ criterion (*Eq. 5*), the two-objects problem should be separated into two independent 1-degree-of-freedom problems. However, solving the problem for one object deter-

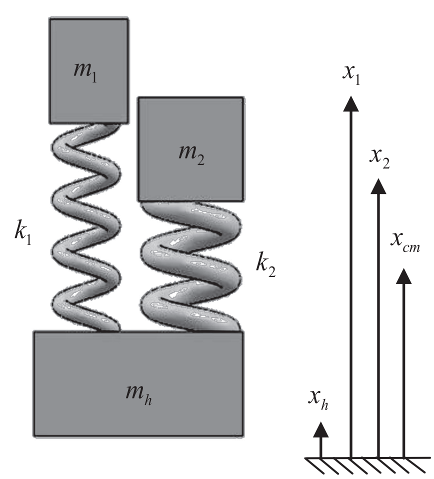

Fig. 3. Diagram of the hand as a point mass, m_h, while attached to 2 external masses, m_1 and m_2, with 2 springs with constants k_1 and k_2. This setup generates 2 masses-on-springs connected to the hand in a parallel way. The hand position is denoted by x_h, the first object position is denoted by x_1, and the second object position is denoted by x_2. The center of mass, x_{cm}, is derived as a weighted sum of the hand position and the object position. This system demonstrates a situation in which the movement of each object depends on the movement of the hand and there is no direct link between the 2 objects.

mines the movement of the other objects, which does not necessarily satisfy the boundary conditions. Therefore, the MHJ model cannot be extended to account for this task.

Minimum object crackle. If we use the MOC model to describe the first mass, the model will satisfy the boundary conditions for the first object and for the hand, leaving yet again the problem of the unsatisfied boundary conditions for the second object. Applying the criterion to both masses can create conflict with the hand trajectory in cases where the ratios between each external mass and its spring are not equal, i.e., $m_1/k_1 \neq m_2/k_2$. Therefore, the MOC model cannot be extended to account for this task.

Minimum acceleration of center of mass. As for simple object manipulation, the MACM model is based on describing the trajectory of the system's CoM using the MACC model, i.e., the CoM trajectory can be described as a straight line with a bell-shaped velocity profile. We can calculate the link between the CoM and the first mass position:

$$x_1^{(4)} + \left(\frac{m_h + m_1}{m_h m_1} + \frac{k_2}{m_h} + \frac{k_2}{m_2}\right)\ddot{x}_1 + k_2 k_1 \frac{(m_1 + m_2 + m_h)}{m_2 m_h m_1} x_1 = \frac{k_1}{m_h m_1}(m_1 + m_2 + m_h)\ddot{x}_{cm} + k_2 k_1 \frac{(m_1 + m_2 + m_h)}{m_2 m_h m_1} x_{cm} \quad (21)$$

Because the position, velocity, and acceleration of the first object and hand are continuous and differentiable, the third and forth derivatives of the first object position exist, i.e., $\dddot{x}_1$ and $x_1^{(4)}$. This can be proved by calculating the limit of the difference quotient using *Eq. 15* (Apostol 1967).

Solving the ordinary differential equation in *Eq. 21* will generate a solution that satisfies the boundary conditions of *Eq. 19*. Using this solution, we can calculate the trajectory of the hand while satisfying the boundary conditions at the beginning and end of the movement. Once the hand, first mass, and CoM trajectory are set, there is no need for special calculation of the second mass trajectory because it is automatically given from the CoM definition:

$$x_{cm} = \frac{m_h x_h + m_1 x_1 + m_2 x_2}{m_h + m_1 + m_2} \quad (22)$$

Similarly, the MACM can be further extended to multiple objects and various external degrees of freedom.

Subjects, Apparatus, and Protocol

Twelve subjects (7 males, 5 females, ages 23–28 yr) participated in three experiments (*A*, *B*, and *C*) after signing the informed consent form as stipulated by the Institutional Helsinki Committee, Beer-Sheva, Israel. Subjects were seated and used their dominant hand to hold the handle of a PHANTOM 1.5 haptic device (SensAble Technologies), which was used to generate real-time forces. The subject looked at a projection screen displaying the virtual environment from a projector placed horizontally above it (Fig. 1*A*). Movements were performed in one dimension by setting limitations on the subject hand, using forces in the direction orthogonal to the movement line. The orthogonal forces were generated according to $F_z(t) = -200 \cdot z_h(t)[N]$, where z_h represents the hand position in the lateral direction (Fig. 1*B*). These forces created an infinitesimal channel for subjects to move, ensuring a straight line movement. After a few trials, all subjects generated straight line movements, so the forces generated orthogonal to the moving direction were unnoticeable. The experiment started with 50 reaching movements between the initial position and the target, the "reaching stage," to familiarize the subject with the system, followed by 900 movements performed while attached to the mass-on-spring, the "object manipulation stage." The mass and spring constants changed during the experiment every 300 trials: the subject interacted with a 2-kg object and a spring with 60 N/m constant in *experiment A*, with a 3-kg object and a spring with 90 N/m constant in *experiment B*, and with a 4-kg object and a spring with 120 N/m constant in *experiment C*. The order of experiment appearance was randomized between subjects (Table 1). In all three experiments the desired movement duration (T) was 1.5 s while the desired movement length (L) was set to 15 cm, i.e., the initial position and target position were 15 cm apart. Subjects could not see their hand, but their hand location was represented by a gray square. To start the movement, subjects needed to set their hand at the initial point by moving the gray square to a blue disk representing the initial position. Once at rest at the initial point, a go signal was given and the subject moved his/her hand to the target, represented by a green disk. During the reaching stage, the visual display of the experiment consisted of these three elements: the hand, the initial point, and the target point. During the object manipulation stage, the subject received additional visual feedback of the mass location from an additional red square, setting the total number of elements to four: the hand (gray square), the object (red square), the initial point (blue disk), and the target point (green disk), as depicted in Fig. 1*A*. The position of the external mass was calculated online by solving the object motion equation (*Eq. 1*). The solution depends on the subject hand position and was calculated using the fourth-order Runge-Kutta method. Hand position was sampled at 1 kHz; therefore, the object position was calculated and forces were rendered at the same rate.

During the object manipulation stage, a trial was considered to be successful *1*) once the subject hand and mass reached the target ($L \pm 0.006$ m); *2*) when at the target point, the velocity of the hand and the mass were very close to complete stop (speed $<$0.006 m/s); and *3*) the movement was performed within a time limit of 1.3–1.7 s. Subjects were given visual feedback as to whether their movements were appropriate, too slow if they did not reach the objective by the desired time, or too fast if they reached the objective before the desired time. Once subjects were given visual feedback about their movement speed, both haptic feedback and visual feedback of the virtual object position were turned off until a new trial was presented.

This procedure was reproduced on 2 consecutive days, setting the total number of movements each subject performed to 1,900 trials: 100 reaching and 1,800 object manipulation (600 trials in each experiment). Subjects were not aware of the changes in spring and mass values, and none reported a feeling of such changes after the experiment ended. Note that although the mass and spring values changed between experiments, the ratio between them, i.e., m_o/k, did not change and was always equal to 1:30.

Data Analysis

Model comparison with the current experiments. To compare the suggested models with experimental data, we took the last 10 successful hand velocity profiles executed by each subject in each

Table 1. *Order of presentation of each of the three experiments*

	Order of Presentation of Experiments		
Subject	First	Second	Third
S1	A	B	C
S2	A	B	C
S3	A	C	B
S4	A	C	B
S5	B	A	C
S6	B	A	C
S7	B	C	A
S8	B	C	A
S9	C	A	B
S10	C	A	B
S11	C	B	A
S12	C	B	A

Experiments A, B, and *C* were presented to subjects in a randomized order.

experiment, i.e., *experiments A*, *B*, and *C* during the second day, and calculated the average velocity profile. To generate model predictions, we used all the parameters set in each of the experiments, i.e., object mass, spring constant, and movement length, identical to the process described by Dingwell et al. (2004). Two of the suggested models, the MHFC model and the MACM model, depend on the mass of the hand. We used predictive regression equations based on anthropometric measures, meaning segment lengths, circumferences, breadths and skin folds (Arthurs and Andrews 2009), to estimate the mass of the hand for each subject. The regression equations we used were tested by Arthurs and Andrews (2009) against actual mass values obtained using dual-energy X-ray absorptiometry scans and showed high success in predicting the hand mass.

To fit the models to the averaged trajectory, we had to obtain the movement duration and movement onset time. As mentioned in the report by Dingwell et al. (2004), subjects may attempt to move with an internal "desired" T that may be shorter than the required time and therefore may obtain more time to dampen extraneous oscillations at the end of the movement and thus still complete the task "successfully." Therefore, it was necessary to vary movement time (T) in fitting the models to the data.

There are many methods for movement onset detection (Botzer and Karniel 2009; Georgopoulos et al. 1982). Here, instead of detecting the onset of movement, for each model the best fit for each averaged trajectory, in the sense of highest explained variance (R^2), was obtained by selecting the best temporal translation and best movement duration. Therefore, all the predicted trajectories from each model compared in this study are the result of fitting these two parameters.

After the best fitted trajectory was obtained, values of the variance accounted for (VAF) were calculated across subjects and experiments and compared. The values of VAF are bounded in [0,100], regardless of the specific experiment. Therefore, we used the nonparametric Friedman's test (Friedman 1937) to determine whether the difference between the VAF values of the models is statistically significant. We used the Wilcoxon signed-rank test for multiple comparisons to perform the comparisons between the individual models.

Model comparison with previous results. In comparing the MACM model predictions with previous results (Fig. 2 of Dingwell et al. 2004), we used the same parameters fitted originally for all the models (movement onset and movement duration) and graphically superimposed these predictions on the original velocity profiles. Because there was no documentation regarding the hand mass in the original article, we choose the hand mass based on the mean value reported by Arthurs and Andrews (2009).

RESULTS

A New Model for Trajectory Formation: MACM

We have derived a new model for trajectory formation (*Eq. 13*), analytically proved (see METHODS) to account for reaching as well as object manipulation. This model describes the optimal trajectory of the hand and is derived from the MACC model for reaching movements without the need to minimize additional criteria considering the new system, which consists of the hand and mass-on-spring.

The model well accounts for previous experimental results. Compared with previously reported experimental results, the MACM model can account for reaching movements without an external object. The MACM model converges to the MACC model when the object mass and spring constant are set to zero, and the ability of the MACC model to accurately predict the characters of simple reaching movements was demonstrated by others (Ben-Itzhak and Karniel 2008; Berret et al. 2011; Yazdani et al. 2012). Therefore, the prediction by the MACM is also consistent with the experimental data as reported in these studies.

In addition to reaching movements, the MACM model can account for previous simplified object manipulation tasks. We examined the results of *experiment B* in Dingwell et al. (2004). This movement was performed by subjects while transferring a 3-kg object with 120 N/m spring between points located 12.5 cm apart. As shown in Fig. 4*A*, the MACM model predicts the typical subject velocity profile for the 1.7-s duration as reported by (Dingwell et al. 2004). In addition, the model can account for the one subject who was not "typical" and showed an irregular velocity profile, as shown in Fig. 4*B*.

The model well accounts for new experimental results. All three experiments tested the MACM model predictions of the object manipulation task compared with previous suggested models while keeping the ratio between the external mass and spring constant. In *experiment A*, all 12 subjects exhibited a biphasic hand velocity profile. The predictions of the MACM model were not significantly different from those of the MOC or MHFC models (Wilcoxon signed-rank test, $P > 0.1$) and significantly better than those of the MHJ model (Wilcoxon signed-rank test, $P < 0.001$). The VAF values for the fitting for each model are presented in Fig. 5*B*, and an example of a velocity profile and fitting is presented in Fig. 5*A*. In *experiments B* and *C*, all 12 subjects again exhibited biphasic hand

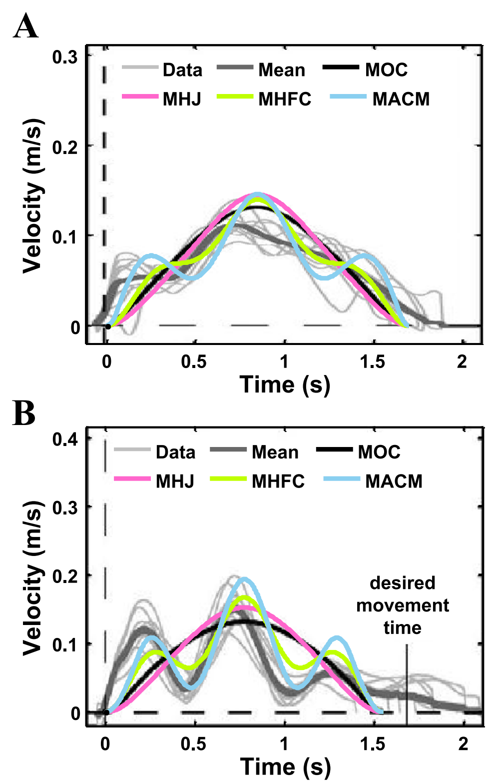

Fig. 4. Models fit to previous results. *A*: typical velocity profile of subjects performing the object manipulation task while transferring a 3-kg object with 120 N/m spring between points located 12.5cm apart (Dingwell et al. 2004). Thin light gray lines represent individual trials, whereas the thick gray line represents the average of these trials. Optimal trajectories predicted by the models are denoted by a black line (minimum object crackle; MOC), pink line (minimum hand jerk; MHJ), green line (minimum hand force change; MHFC), and blue line (minimum acceleration of center of mass; MACM). *B*: velocity profile of the exceptional subject reported by Dingwell et al. (2004). Lines are as described in *A*. [Both *A* and *B* were modified from Dingwell et al. (2004).]

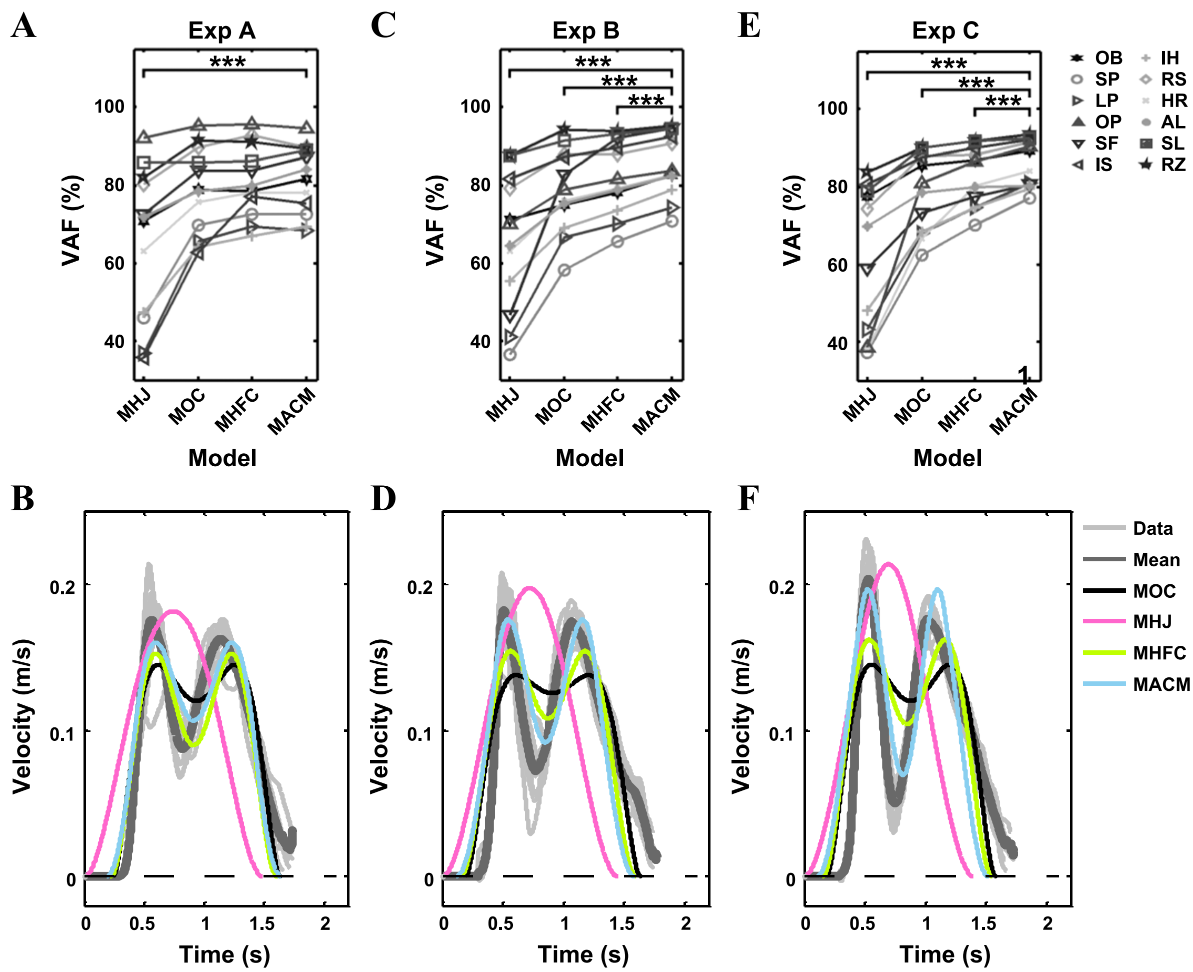

Fig. 5. Models fit to new experimental results. *A*: individual variance accounted for (VAF) by each model in *experiment A*. ***$P < 0.001$ indicates significant difference (see RESULTS). *B*: velocity profile for a single subject from *experiment A*. Thin light gray lines represent individual trials, whereas thick gray line represents the average of these trials. Optimal trajectories predicted by the models are denoted by a black line (MOC), pink line (MHJ), green line (MHFC), and blue line (MACM). *C*: individual VAF values in *experiment B*. *D*: velocity profile for a single subject from *experiment B*. *E*: individual VAF values in *experiment C*. *F*: velocity profile for a single subject from *experiment C*.

velocity profiles. The predictions of the MACM model were significantly better than those of the MOC, MHJ, and MHFC models (Wilcoxon signed-rank test, $P < 0.001$). The VAF values for the fitting for each model are presented in Fig. 5, *D* and *F*, and examples of the respective velocity profiles and fittings are presented in Fig. 5, *C* and *E*. The success rates of each subject were also similar across experiments, ranging between 34% and 72%. Fitted movement times (T) were similar across experiments for each model (in s): MHJ, mean 1.424 (SD 0.184); MOC, mean 1.336 (SD 0.160); MHFC, mean 1.417 (SD 0.182), and MACM, mean 1.531 (SD 0.197). The differences between actual movement duration performed by subjects and the fitted movement duration for each model were as follows (in s): MHJ, mean 0.122 (SD 0.015); MOC, mean 0.132 (SD 0.023); MHFC, mean 0.118 (SD 0.01); and MACM, mean 0.089 (SD 0.026).

Next, we tested whether the hand mass is related to kinematic features exhibited by the subjects. We tested the correlation between the hand mass and local minimum and maximum values of the velocity profile. We found negative correlation between hand mass and the mean local maximum value of the velocity profile exhibited in the three experiments (Pearson $r = -0.743$, $P = 0.021$) and positive correlation between hand mass and the mean local minimum value of the velocity profile exhibited in the three experiments (Pearson $r = 0.717$, $P = 0.045$). These results show that kinematic features of the movement change with hand mass as predicted by the MACM and MHFC models.

DISCUSSION

In this study we derived a computational model for object manipulation based on the minimum acceleration with constraints criterion applied to the center of mass (MACM). We used a known paradigm to simulate a mass-on-spring system and showed that minimizing the hand-mass system CoM acceleration can account for our observed experimental data. We considered three additional models and found that the MACM can explain the results better than these previous models. Moreover, we showed that unaccountable previous results, regarded as not typical, are well accounted for by our model.

The criterion of minimum acceleration was found successful for reaching movement, and here we show a generalization of this criterion for mass-on-spring manipulation. During our experiments we changed the values of the external mass and spring constant but kept the ratio between these two elements constant. This was done to check whether the hand kinematic changes, as we did see, but limited our possibilities to learn about the ability to generalize to different mass-on-spring objects. The constant ratio sets the same dynamic equation for the external object, making it possible for the subject to generalize between the objects we presented but keeping the question of generalizing to different object dynamics still open (Dingwell et al. 2002). To further test our model, we can examine the generalization of the present solution to different mass-on-spring dynamics and different tasks (e.g., reaching with a glass full of water, flexible or articulated rods, etc.).

As suggested by Svinin et al. (2006), the ability of a model to be extended to more complex environments can show advantages of one criterion over the other. We showed that the solution for simple point-to-point reaching movement can be used to generate the needed movement during transport of a mass-on-spring object without the need for resolving the optimization problem. With the use of this procedure, the model can be extended even further to more complex environments with more degrees of freedom, such as a chain of masses connected by springs (Svinin et al. 2006) or multiple masses-on-springs connected in a parallel way. The extension of other models to the later mentioned environment is not as trivial, if even possible, as we showed in METHODS.

Our model is based on three underlying principles: *1*) minimum acceleration as the optimization criterion, *2*) the CoM as the relevant variable, and *3*) maximum CoM jerk as a constraint. Because the MACM model, as well as the other models, describes the endpoint trajectory, it is independent of manipulation goal and other task parameters such as the movement direction. The CoM jerk constraint, u, found during the model derivation process in *Eq. 13*, is used to satisfy a continuity condition, eliminating the possibility of a discontinuous hand velocity profile. Setting the CoM jerk to a different value would generate a discontinuous point in the hand velocity profile, which implies an unbounded, nonsmooth, and nonphysiological hand acceleration profile. It is important to note that the question of the underlying principle on which movements are planned is still open. The previous criteria, such as MHJ and MHFC, need to be converted from hand coordinates to object coordinates to be calculated. The equivalency between these criteria (*Eqs. 5* and *6* and *Eqs. 7* and *8*) make it harder to determine which formulation the central nervous system is using. In our system, minimizing the acceleration of the CoM is equivalent to minimizing the hand driving force. Similarly, the minimum jerk of the CoM is equivalent to the MHFC as mentioned in *Eq. 7*. This is easy to prove by examining the definitions of the MACM and minimum hand force cost functions, $\int_0^T [F]^2 \mathrm{d}t$, while keeping in mind the definition for the CoM and the dynamic equations of the system (see *Eqs. 1*, 2, and *9*). The equality between the MACM and minimum hand force makes it difficult to determine whether the hand trajectory is the outcome of minimizing the CoM acceleration or the CoM trajectory is the outcome of minimizing the driving forces of the hand during movement. As further discussed below, planning and executing movements in the task space of CoM coordinates may reflect a general approach with metabolic benefits that can be extended and tested in more sophisticated object manipulation tasks.

We propose a model for the arm trajectory after extended training. One should note that in the practice session, subjects have to learn the task using dynamic and kinematic information (Krakauer et al. 1999). Visual and proprioceptive information about the hand and object states as well as the forces acting during movement are required to form an internal representation of the external system (Izawa et al. 2008). Because the dynamics of the hand are changed with the additional external mass and the kinematic planning is changed by the multiple objectives, subjects need to learn the new environment. The learning process is evident from the increased success rate of keeping within the demands of the mass-on-spring transporting task (Svinin et al. 2006) or by the shortening of the movement duration (Dingwell et al. 2002). In this sense our model suggests that subjects need to both estimate the dynamics changes, i.e., the altered CoM, and use different kinematic planning, i.e., implicitly compute the required hand movement that will create CoM trajectory with similar characteristics of the unconstrained reaching movement.

Previous studies supported the ability of subjects to estimate the CoM by using vision (Hirsch and Mjolsness 1992; Salimi et al. 2003) and the size of objects (Friedenberg and Liby 2002). Proprioceptive information may provide a sense of forces acting on the hand during movement; however, because trajectory planning is predictive, the nervous system can use sensory information from the previous trial to predict other variables such as the CoM. Because both hand and mass were presented as squares with the same size, it is not inevitable that there was integration of proprioceptive and visual feedback to estimate the CoM.

The CoM variable appears to be relevant to the motor system for a range of activities. Most relevant to this work is the possibility of the CoM to have fundamental rule in planning reaching movements (Suzuki et al. 1997). Other examples can be found in studies of limb orientation perception (van de Langenberg et al. 2007), body orientation perception (Fourre et al. 2009), sit-to-stand tasks (Scholz and Schöner 1999), or object grasping tasks (Lukos et al. 2007). Furthermore, controlling the CoM variable may affect metabolic cost, for example, during walking (Gordon et al. 2009). We provide another role for the CoM as the controlled variable during transport of flexible objects; our setup focused on one-dimensional (1-D) movement, where there is only one geometrical solution corresponding to the CoM position while the number of fingers holding the robotic handle or the way it is grasped is made irrelevant to the task goal. Future studies could further test our model in 2-D and 3-D movement and extend it to various hand-grip configurations.

An important prediction of the MACM model is an intermittence control, because the solution is divided into three parts. Intermittence is particularly useful for hierarchical systems with delay (Gawthrop et al. 2011). This view of the neural control of movement suggests that the central nervous system sends sparse command to the spinal cord to switch motor command at certain points of time, such as the three points in our solution.

As previously suggested, the internal representation of objects can be related to the cerebellum (Nowak et al. 2007). In the structure of internal models (Kawato 1999), the cerebellum is linked with the role of a forward model (Pasalar et al. 2006) because it may have the ability to predict movement outcome. In the context of object manipulation, the cerebellum may have to acquire the intrinsic dynamics of the object to predict how hand movements and generated forces will affect the object movement, as seen, for example, when learning to use a new tool (Imamizu et al. 2000). This new model has interesting implications about the possible neural representation of the CoM, together with the intermittent nature of the control and its relation to neural bursts such as the bistability observed in Purkinje cells (Loewenstein et al. 2005).

In this study we derived a model for both reaching and simplified object manipulation tasks. This new model extends the minimum acceleration with constraints model, suggesting that during simple reaching movements and object manipulation, the state variable being controlled is the center of mass. Because the controlled variable and the optimization criteria do not change between tasks, the suggested solution creates the desirable simple strategy for the brain to implement during daily interaction with the environment.

GRANTS

This research was supported by Israel Science Foundation Grant 1018/08.

DISCLOSURES

No conflicts of interest, financial or otherwise, are declared by the authors.

AUTHOR CONTRIBUTIONS

R.L. and A.K. conception and design of research; R.L. performed experiments; R.L. analyzed data; R.L. and A.K. interpreted results of experiments; R.L. prepared figures; R.L. drafted manuscript; R.L. and A.K. edited and revised manuscript; R.L. and A.K. approved final version of manuscript.

REFERENCES

Abend W, Bizzi E, Morasso P. Human arm trajectory formation. *Brain* 105: 331–348, 1982.

Apostol TM. *Calculus: One-Variable Calculus, With an Introduction to Linear Algebra*. Waltham, MA: Blaisdell, 1967.

Arthurs KL, Andrews DM. Upper extremity soft and rigid tissue mass prediction using segment anthropometric measures and DXA. *J Biomech* 42: 389–394, 2009.

Ben-Itzhak S, Karniel A. Minimum acceleration criterion with constraints implies bang-bang control as an underlying principle for optimal trajectories of arm reaching movements. *Neural Comput* 20: 779–812, 2008.

Berret B, Chiovetto E, Nori F, Pozzo T. Evidence for composite cost functions in arm movement planning: an inverse optimal control approach. *PLoS Comput Biol* 7: e1002183, 2011.

Botzer L, Karniel A. A simple and accurate onset detection method for a measured bell-shaped speed profile. *Front Neurosci* 3: 61, 2009.

Boyce W, DiPrima R. *Introduction to Differential Equations*. New York: Wiley, 1970.

Dingwell JB, Mah CD, Mussa-Ivaldi FA. Experimentally confirmed mathematical model for human control of a non-rigid object. *J Neurophysiol* 91: 1158–1170, 2004.

Dingwell JB, Mah CD, Mussa-Ivaldi FA. Manipulating objects with internal degrees of freedom: evidence for model-based control. *J Neurophysiol* 88: 222–235, 2002.

Flash T, Hogan N. The coordination of arm movements: an experimentally confirmed mathematical model. *J Neurosci* 5: 1688–1703, 1985.

Fourre B, Isableu B, Bernardin D, Gueguen M, Giraudet G, Vuillerme N, Pagano C, Amorim MA. The role of body centre of mass on haptic subjective vertical. *Neurosci Lett* 465: 230–234, 2009.

Friedenberg J, Liby B. Perception of two-body center of mass. *Percept Psychophys* 64: 531–539, 2002.

Friedman M. the use of ranks to avoid the assumption of normality implicit in the analysis of variance. *J Am Stat Assoc* 32: 675–701, 1937.

Gawthrop P, Loram I, Lakie M, Gollee H. Intermittent control: a computational theory of human control. *Biol Cybern* 104: 31–51, 2011.

Georgopoulos A, Kalaska J, Caminiti R, Massey J. On the relations between the direction of two-dimensional arm movements and cell discharge in primate motor cortex. *J Neurosci* 2: 1527–1537, 1982.

Gordon KE, Ferris DP, Kuo AD. Metabolic and mechanical energy costs of reducing vertical center of mass movement during gait. *Arch Phys Med Rehabil* 90: 136–144, 2009.

Hirsch J, Mjolsness E. A center-of-mass computation describes the precision of random dot displacement discrimination. *Vision Res* 32: 335–346, 1992.

Hogan N. An organizing principle for a class of voluntary movements. *J Neurosci* 4: 2745–2754, 1984.

Huegel JC, Lynch AJ, O'Malley MK. Validation of a smooth movement model for a human reaching task. In: *ICORR 2009 IEEE International Conference on Rehabilitation Robotics*, 2009, p. 799–804.

Imamizu H, Miyauchi S, Tamada T, Sasaki Y, Takino R, Putz B, Yoshioka T, Kawato M. Human cerebellar activity reflecting an acquired internal model of a new tool. *Nature* 403: 192–195, 2000.

Izawa J, Rane T, Donchin O, Shadmehr R. Motor adaptation as a process of reoptimization. *J Neurosci* 28: 2883–2891, 2008.

Kawato M. Internal models for motor control and trajectory planning. *Curr Opin Neurobiol* 9: 718–727, 1999.

Krakauer JW, Ghilardi MF, Ghez C. Independent learning of internal models for kinematic and dynamic control of reaching. *Nat Neurosci* 2: 1026–1031, 1999.

Loewenstein Y, Mahon S, Chadderton P, Kitamura K, Sompolinsky H, Yarom Y, Hausser M. Bistability of cerebellar Purkinje cells modulated by sensory stimulation. *Nat Neurosci* 8: 202–211, 2005.

Lukos J, Ansuini C, Santello M. Choice of contact points during multidigit grasping: effect of predictability of object center of mass location. *J Neurosci* 27: 3894–3903, 2007.

Morasso P. Spatial control of arm movements. *Exp Brain Res* 42: 223–227, 1981.

Nowak D, Topka H, Timmann D, Boecker H, Hermsdörfer J. The role of the cerebellum for predictive control of grasping. *Cerebellum* 6: 7–17, 2007.

Pasalar S, Roitman AV, Durfee WK, Ebner TJ. Force field effects on cerebellar Purkinje cell discharge with implications for internal models. *Nat Neurosci* 9: 1404–1411, 2006.

Salimi I, Frazier W, Reilmann R, Gordon AM. Selective use of visual information signaling objects' center of mass for anticipatory control of manipulative fingertip forces. *Exp Brain Res* 150: 9–18, 2003.

Scholz JP, Schöner G. The uncontrolled manifold concept: identifying control variables for a functional task. *Exp Brain Res* 126: 289–306, 1999.

Suzuki M, Yamazaki Y, Mizuno N, Matsunami K. Trajectory formation of the center-of-mass of the arm during reaching movements. *Neuroscience* 76: 597–610, 1997.

Svinin M, Goncharenko I, Zhi-Wei L, Hosoe S. Reaching movements in dynamic environments: how do we move flexible objects? *IEEE Trans Robot* 22: 724–739, 2006.

Svinin M, Masui Y, Luo ZW, Hosoe S. On the dynamic version of the minimum hand jerk criterion. *J Robot Syst* 22: 661–676, 2005.

Uno Y, Kawato M, Suzuki R. Formation and control of optimal trajectory in human multijoint arm movement. *Biol Cybern* 61: 89–101, 1989.

van de Langenberg R, Kingma I, Beek P. Perception of limb orientation in the vertical plane depends on center of mass rather than inertial eigenvectors. *Exp Brain Res* 180: 595–607, 2007.

Yazdani M, Gamble G, Henderson G, Hecht-Nielsen R. A simple control policy for achieving minimum jerk trajectories. *Neural Netw* 27: 74–80, 2012.